Asymmetric Spatial Beams with Symmetric Kinetostatic Behaviour

Amoozandeh Nobaveh, Ali; Radaelli, Giuseppe; Herder, Just L.

DOI
10.1007/978-3-030-58380-4_30

Publication date
2021

Document Version
Accepted author manuscript

Published in
Proceedings ROMANSY 23 - Robot Design, Dynamics and Control

Citation (APA)
Amoozandeh Nobaveh, A., Radaelli, G., & Herder, J. L. (2021). Asymmetric Spatial Beams with Symmetric Kinetostatic Behaviour. In G. Venture, J. Solis, Y. Takeda, & A. Konno (Eds.), *Proceedings ROMANSY 23 - Robot Design, Dynamics and Control* (pp. 247-254). (CISM International Centre for Mechanical Sciences, Courses and Lectures; Vol. 601). Springer. https://doi.org/10.1007/978-3-030-58380-4_30

Important note
To cite this publication, please use the final published version (if applicable).
Please check the document version above.

Asymmetric Spatial Beams with Symmetric Kinetostatic Behaviour *

Ali Amoozandeh Nobaveh[1][0000−0002−0722−6550], Giuseppe Radaelli[1][0000−0002−2935−3868], and Just L. Herder[1][0000−0002−2770−0539]

Precision and Microsystems Engineering Dept., Delft University of Technology, 2628CD, Delft, The Netherlands
A.AmoozandehNobaveh@tudelft.nl

Abstract. A method to achieve symmetric kinetostatic behaviour in an extensive working range at the endpoint of an asymmetric spatial beam, using cross-section optimization, is presented. The objective function of the optimization is defined as expanding the beam working range to the desired region, simultaneously maximizing symmetric behaviour in it. To reach this goal, a beam with predefined spatial global shape and an 'I' cross-section selected. The cross-sectional dimensions throughout the beam are used as input values for the optimization. The endpoint displacements under symmetric loadings are attained using a nonlinear co-rotational beam element based on the Euler-Bernoulli beam formulation. The optimized beams are compared to a circular cross-section beam with the same global shape to show the efficacy of the method. Isoforce diagrams are investigated for the optimized beams to show the symmetry behaviour of the beam endpoint and the effect of changing different parameters in cross-sectional optimization is discussed.

Keywords: Spatial compliant mechanism · Asymmetric beam · Symmetric stiffness · Cross-section optimization · Isoforce mapping

1 Introduction

The ability to design spatial elastic elements with a predetermined kinetostatic character, i.e. the integration of the function of kinematic and spring elements, is desirable in several application domains. In wearable device technology, for example, it is imperative to design parts that are able to apply support forces to the body in concordance with specific kinematics of the limbs. It is presumably redundant to say that other application domains may partially profit from these functional requirements as well, ranging the entire spectrum of application of robotics and mechanisms.

In recent years, spatial compliant mechanisms have increasingly been the topic of interest in the mechanism design community. Efforts have been made in both the characterization as in the design and optimization of spatial compliant mechanisms for the sake of advancing their applicability as full devices

* Supported by NWO (P16-05: Shell Skeletons)

or as components. In flexures, which are flexible elements widely used for precision mechanisms, there are plenty of examples of spatial mechanisms [6,10] and established design principles exist [4,12].

In these applications the kinematic requirement is leading, i.e. the contrast in stiffness between free and constraint directions must be extreme, on the other hand, ranges of motion are often small and the spatial occupation of the mechanism is not restrictive. This often leads to the employment of straight or notch flexures, in relatively complex spatial orientations and topologies with many parallelly connected kinematic chains. Examples of spatial compliant mechanisms with large ranges of motion and simpler topologies, e.g. [2, 7–9, 11, 13, 14], are emerging, but scarcer.

From an utilization perspective as well as from a fabrication perspective, it appears convenient to consider an utmost simple topology of a cantilevered spatial beam, that is, a beam clamped at one end and loaded at its opposite end. The peculiar kinetostatic behaviour sought in this work is one where the spatial beam has a plane symmetry of loading forces and corresponding endpoint displacements, while the geometry of the beam itself is not symmetric with respect to the same plane. This type of behaviour has not been found by the authors in any earlier work. On the other hand, it is expected to be useful in distinct applications where the plane or area of action of the end-effector does not coincide with the available grounding positions. This is true for manipulator-type devices, where the ground attachment point must not interfere with the end-effector range of motion, and also in wearable devices where the symmetry plane of the body is to a large extend occupied by the body itself.

The usual behaviour of whichever spatial beam is that upon loading the free end with a force, it somehow turns about the ground attachment point as a result of the moment produced by that force. It is hypothesised that there exist non-uniform distributions of cross-sectional properties for which the natural turning behaviour of the beam is corrected towards a more planar motion.

This paper presents an asymmetric spatial cantilevered beam with a semi-symmetrical kinetostatic behaviour, generated by optimization of cross-sectional properties of a given global beam shape. The cross-sectional shape is chosen to be a conventional I-profile. The symmetric behaviour is optimized by minimizing the differences in point-pairs displacements under symmetric loading about the desired plane. The beam displacements are computed numerically with a finite element model for beams, suitable for large displacements.

The paper is structured as follows. In section 2 the definition of the global geometry of the beam is given together with the description of the cross-sectional parameters to be optimized, the formulation of the objective function and the optimization settings. In section 3 the results are shown and compared to the non-optimized beam. A discussion on the validity and applicability of the results and possible improvements is given in section 4, and the conclusion is given in section 5.

2 Methods

The global undeformed beam shape (see Fig. 1a), could be chosen arbitrarily and will not be subject to optimization. In this particular case the reference axis of the beam is parametrized as

$$(x, y, z) = (C_1 t^3,\ a - b(C_2 t - c)^2,\ C_3 t), \tag{1}$$

where t is the independent parameter ranging from 0 to 40, the constants a, b and c are chosen as $a = 1.5, b = 0.75, c = \sqrt{2}$, and the constants C_1, C_2 and C_3 are determined such that the end of the beam reaches the arbitrarily chosen coordinates $X_e = 0.20\,\mathrm{m}$, $Y_e = 0.15\,\mathrm{m}$ and $Z_e = 0.50\,\mathrm{m}$. This is achieved by satisfying the relations

$$C_1 = \frac{X_e}{t^3}, \quad C_2 = \frac{\sqrt{\frac{a - Y_e}{b}} + c}{t}, \quad C_3 = \frac{Z_e}{t}. \tag{2}$$

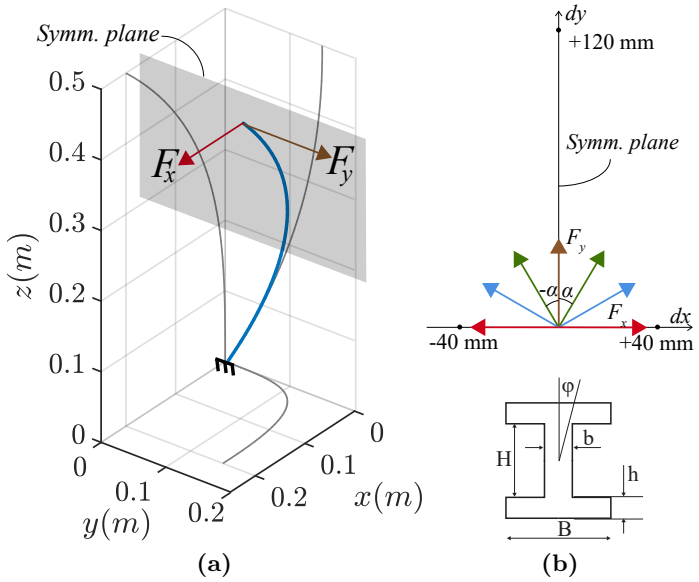

Fig. 1. (a) The global shape of the beam and its projections on the main planes, (b) parameters of the 'I' cross-section, and symmetric loadings in desired working range of the beam.

The beam is clamped at the lower end and is loaded by force F at the endpoint. The magnitude of the force, is kept constant, and the components of the force vary with the angle α, defined from the plane of desired symmetry, as

$$(f_x, f_y, f_z) = (F \sin\alpha, F \cos\alpha, 0). \tag{3}$$

The defined objective function f for the optimization procedure includes two parts f_1 and f_2. The first part, f_1, consists of the average of displacement differences in the three Cartesian coordinates for a number of point-pairs, resulting from a mirrored loading condition with a force magnitude of $F = 100\,\mathrm{N}$ and an angle of $\pm\alpha$, where $\alpha = 30°$, $60°$, and $90°$. This error part is named symmetry error. This part of the objective assures a degree of symmetry of the kinetostatic response within the region reached by the applied forces. However, that region might be unsatisfactory in terms of in-plane and out-of-plane displacement magnitudes, i.e., the resulting symmetry could be achieved only in minimal displacement ranges or in narrow bands of offset from the symmetry plane. For this reason, a second part of the objective, f_2, is defined. The second part considers the error of the end point displacement under the loadings in the x and y directions concerning chosen working range, in this case, $0.12\,\mathrm{m}$ in the y direction and $0.04\,\mathrm{m}$ in the x direction (see Fig. 1b). This error part is named range error. The total objective function is an unweighted summation of the above-mentioned parts and is defined as

$$\begin{aligned} f = f_1 + f_2 = \Big(\sum_{\alpha=30,60,90} \frac{1}{3}\big(|dx_{+\alpha} - dx_{-\alpha}| + |dy_{+\alpha} - dy_{-\alpha}| + |dz_{+\alpha} - dz_{-\alpha}|\big)\Big) \\ + \big(|0.04 - dx_{\alpha=90}| + |0.12 - dy_{\alpha=0}| + |dx_{\alpha=0}|\big), \end{aligned} \tag{4}$$

where α is the effective angle of F and dx, dy, dz are displacements in the three coordinate directions. The optimization procedure is assigned to minimize the mentioned objective function by optimizing the cross-sectional properties of the described beam. In principle, it is possible to choose any cross-section for the spatially curved beam. However, the I-shaped cross-section is selected among prevalent commercial cross-sections, since changing its parameters enables a large variety of combinations of second moments of inertia in the two main axes, and the torsional constant. The cross-sections are doubly symmetric and are defined by their web height H, flange width B, flange thickness to web height ratio $\tilde{h} = h/H$, web thickness to flange width ratio $\tilde{b} = b/B$, and the orientation ϕ (see Fig. 1b). The cross-section parameters are optimized at N main cross-sections (see Fig. 3) and interpolated by a B-spline to find out all other cross-section properties along the beam length. The employed interpolating B-spline is a degree-four for five or more cross-section and degree-two for three cross-sections, associated with an open uniform knot vector with its internal knots determined based on de Boor algorithm [5]. This knot vector ensures that the parameters of the first and last optimized cross-sections coincide with the first and last cross-sections of the beam itself. It is important to note that optimizing all cross-sections separately could lead to more promising results. However, it would cause more expensive computations, and notable dimension discontinuities between the beam elements which make the utilized mechanical model invalid.

The displacements mentioned in eq. (4) are derived from a self-developed finite element solver using geometrically nonlinear co-rotational beam elements introduced by Battini [1], based on a Euler-Bernoulli beam formulation, and the described beam is discretized into forty elements.

For the optimization process, the *Multi Start* option with five random starting points, using the *fmincon* function with the *Interior-Point Algorithm* from the Matlab® *optimization toolbox* is used. The optimization was subject to the bounds on the parameters shown in table 1 as Min and Max. These bounds are set to limit the algorithm to come up with reasonable dimensions and to keep the I-shape through the beam. The material constants used in the model are Young's modulus $E = 200GPa$ and shear modulus $G = 76.9GPa$.

3 Results

To evaluate the method, beams with different optimized cross-sections but identical global shape are subjected to the same loading conditions as elaborated in section 2, and the objectives are compared. To represent the kinetostatic behaviour of the beam, an isoforce mapping [3] is presented. Each isoforce line represents the displacement of the endpoint of the beam subject to a constant magnitude of the force F (see Fig. 1b), with a full cycle of the angle α. This mapping is shown for a reference beam, with circular cross-section and optimized radius of 5.4 mm, (see Fig. 2a and 2d). The red points on the x and y axis represent the positions of the desired displacements when the force is applied only in the x and y directions respectively, while the blue points represent the actual displacements obtained when the beam is subjected to these loadings. The green dashed lines connect the displacement of pairs of points, i.e., with opposite angle α of force F, within the optimized region. It also shows the cross-sections, in the undeformed and deformed configurations. This figure illustrates how straight the endpoint of the beam moves subject to a force in the y direction only (see Fig. 1a). It can be observed that with a circular cross-section the desired displacement is poorly achieved and that a force in the y direction results in a notable lateral drift. Similar figures are provided (see Fig. 2b,e and Fig. 2c,f) for an I-beam with a uniform optimized cross-section ($N = 1$), and another I-beam with five optimized main cross-sections ($N = 5$). The optimized parameters are given in Table 1.

An analysis of the impact of the number of optimized cross-sections on the resulting objective was performed (see Fig. 3). Also, as a benchmark, the objective achieved by a uniform circular cross-section is shown to highlight the performance leap obtained by the optimization effort.

4 Discussion

The improvements on the symmetry behaviour obtained by optimizing cross-sectional parameters across the I-beam are significant (see Figs. 2b and 2c) as compared to circular beam. The obtained displacements have a undoubtedly

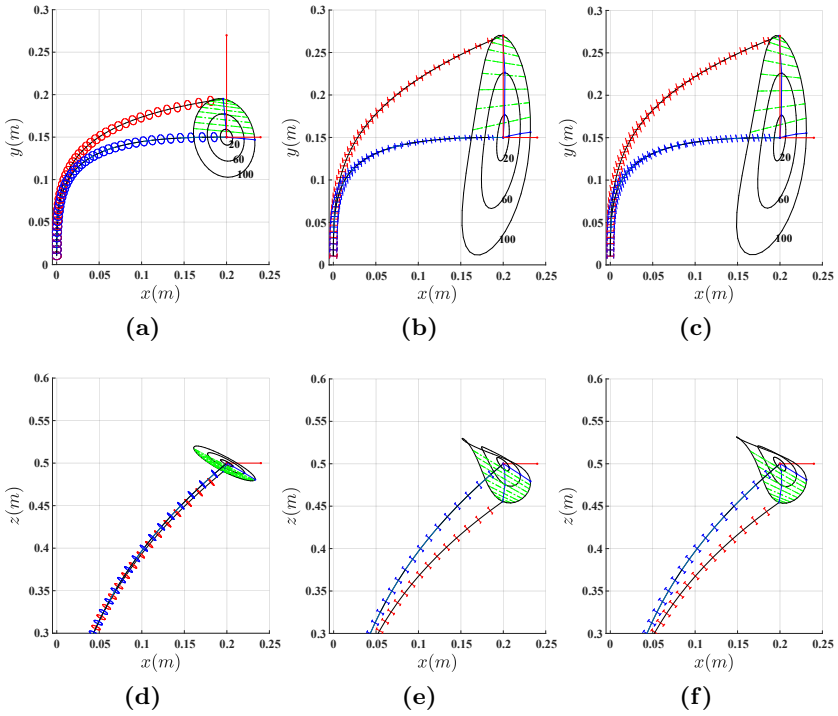

Fig. 2. Isoforce mapping in the desired range, (a,d) circular beam top and rear view (b,e) uniform 'I' cross-section beam top and rear view (c,f) non-uniform 'I' cross-section beam top and rear view. Cross-section dimensions are mentioned in Table 1.

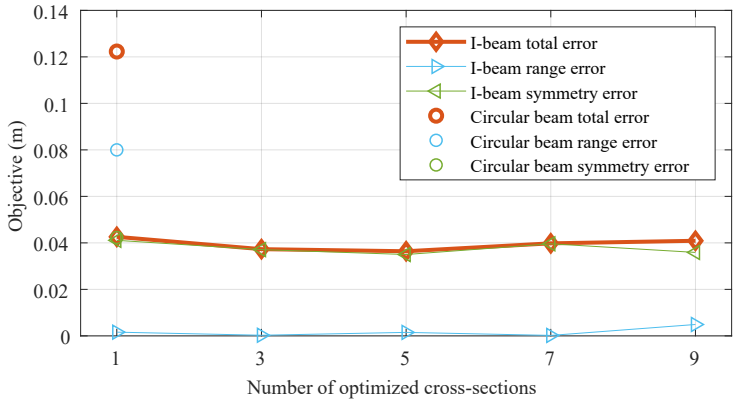

Fig. 3. Objective function for circular, uniform and non-uniform optimized 'I' beam.

Table 1. Optimized parameters for uniform cross-section and non-uniform cross-sections optimization with bounds.

Parameter	Min	Max	CS	CS-1	CS-2	CS-3	CS-4	CS-5
H(mm)	4	8	5.75	5.4	6.1	6.3	6.3	6.2
B(mm)	6	12	6.77	6.5	7.6	8.8	9.2	9.2
$\tilde{h}$	0.2	0.8	0.46	0.47	0.48	0.53	0.55	0.53
$\tilde{b}$	0.2	0.8	0.79	0.64	0.58	0.54	0.51	0.50
ϕ(deg)	10	170	85.96	89.98	89.99	89.99	90.00	90.00

better match, the region of symmetry is more extended, and the path of the endpoint subject to a force in the y-direction is straighter. It is fair to note that the symmetry in z-direction was not improved with the optimization. Apparently, the effect of the global shape and its inclination is hard to counteract by the cross-section variations allowed by the given model. This also underlines the dependence of the presented results to the initially chosen global shape. The proposed procedure could generally be applied to every global geometry, but the results heavily rely on it. Depending on the flexibility of the design space of the specific problem at hand, it might be recommendable to employ a combined optimization of global shape and cross-sections.

The optimization process shows that increasing the number of optimized cross-sections will not indeed lead to lower errors yet make the problem computationally expensive. This optimal number of optimized cross-sections should be investigated for each desired range and initial conditions.

There are limitations inherent to the employed mechanical model which follow from the Euler-Bernoulli assumptions and from the required symmetry of the cross-sections, of which the effect still has to be investigated. Relieving these assumptions, which suppress all cross-sectional deformations, e.g., shear deformation, warping and in-plane deformation, presumably makes more complex behaviour emerge, possibly allowing an enhanced performance as a result.

5 Conclusion

This paper presents a new method to achieve symmetric kinetostatic behaviour from asymmetric spatial beams using cross-sectional optimization, given a global shape. The global shape could be designed with a specific path or line based on requirements. The effectiveness of this method has been validated by comparing symmetry error and range error of the optimized conventional 'I' beam and circular beam cross-section in a predetermined field. Rather complex cross-sectional properties were found by optimization, using a nonlinear beam element to determine displacement differences between point pairs and minimizing them, which resulted in an symmetric behaviour in a proportionally extensive working range. Such design requirements are not easily achieved with existing methods for compliant mechanism design, which shows the capacity of this method to handle more complex design demands.

References

1. Battini, J.M.: Co-rotational beam elements. Ph.D. thesis, Royal Institute of Technology, Stockholm, Sweden (2002)
2. Bilancia, P., Berselli, G., Bruzzone, L., Fanghella, P.: A CAD/CAE integration framework for analyzing and designing spatial compliant mechanisms via pseudo-rigid-body methods. Robotics and Computer-Integrated Manufacturing **56**, 287–302 (apr 2019). https://doi.org/10.1016/J.RCIM.2018.07.015
3. Doornenbal, B.: Zero stiffness composite shells using thermal prestress, MSc thesis, Delft University of Technology, Delft, The Netherlands (2018)
4. Hopkins, J.B., Culpepper, M.L.: Synthesis of multi-degree of freedom, parallel flexure system concepts via Freedom and Constraint Topology (FACT) – Part I: Principles. Precision Engineering **34**(2), 259–270 (apr 2010). https://doi.org/10.1016/J.PRECISIONENG.2009.06.008
5. Hoschek, J., Lasser, D.: Fundamentals of computer-aided geometric design. A.K. Peters (1993)
6. Howell, L.L., Magleby, S.P., Olsen, B.M.: Handbook of Compliant Mechanisms. Wiley, Somerset, 1 edn. (2013)
7. Nijssen, J.P.A., Radaelli, G., Herder, J.L., Ring, J.B., Kim, C.J.: Spatial Concept Synthesis of Compliant Mechanisms Utilizing Non-Linear Eigentwist Characterization. In: Volume 5A: 42nd Mechanisms and Robotics Conference. American Society of Mechanical Engineers (aug 2018). https://doi.org/10.1115/DETC2018-85307
8. Parlaktaş, V.: Spatial compliant constant-force mechanism. Mechanism and Machine Theory **67**, 152–165 (sep 2013). https://doi.org/10.1016/j.mechmachtheory.2013.04.007
9. Parlaktaş, V., Tanık, E.: Single piece compliant spatial slider–crank mechanism. Mechanism and Machine Theory **81**, 1–10 (nov 2014). https://doi.org/10.1016/J.MECHMACHTHEORY.2014.06.007
10. Rad, F.P., Berselli, G., Vertechy, R., Castelli, V.P.: Compliance based characterization of spherical flexure hinges for spatial compliant mechanisms. In: Advances on Theory and Practice of Robots and Manipulators, pp. 401–409. Springer (2014)
11. Radaelli, G., Herder, J.L.: Study on the large-displacement behaviour of a spiral spring with variations of cross-section, orthotropy and prestress. Mechanical Sciences **9**(2), 337–348 (oct 2018). https://doi.org/10.5194/ms-9-337-2018
12. Turkkan, O.A., Venkiteswaran, V.K., Su, H.J.: Rapid conceptual design and analysis of spatial flexure mechanisms. Mechanism and Machine Theory **121**, 650–668 (mar 2018). https://doi.org/10.1016/J.MECHMACHTHEORY.2017.11.025
13. Weeger, O., Narayanan, B., Dunn, M.L.: Isogeometric shape optimization of nonlinear, curved 3d beams and beam structures. Computer Methods in Applied Mechanics and Engineering **345**, 26–51 (2019)
14. Zhou, H., Ting, K.L.: Geometric Optimization of Spatial Compliant Mechanisms Using Three-Dimensional Wide Curves. Journal of Mechanical Design **131**(5), 051002–051002 (apr 2009). https://doi.org/10.1115/1.3086792